Qualitative and quantitative study of human osteoblast adhesion on materials with various surface roughnesses

Karine Anselme, Maxence Bigerelle, B. Noel, E. Dufresne, D. Judas, A. Iost, P. Hardouin

Qualitative and quantitative study of human osteoblast adhesion on materials with various surface roughnesses

K. Anselme,[1] M. Bigerelle,[2] B. Noel,[1] E. Dufresne,[2] D. Judas,[3] A. Iost,[2] P. Hardouin[1]
[1]*IRMS, Institut Calot, Rue du Dr. Calot, 62608 Berck-sur-Mer, France*
[2]*ENSAM UMR CNRS 8517, 8 Boulevard Louis XIV, 59046 Lille, France*
[3]*CRITT Céramiques Fines, Z.I. Champ de l'Abbesse, 59600 Maubeuge, France*

Abstract: We quantitatively evaluated the adhesion of human osteoblasts on orthopedic metallic substrates (Ti6Al4V alloy) with various surface roughnesses at several times after inoculation and studied its correlation with qualitative changes in the expression of adhesion proteins and with parameters extensively describing the surface topographies. Cells were orientated in a parallel order on polished surfaces. This orientation was not affected by residual grooves after polishing. On sandblasted surfaces the cells never attained confluence and had a stellate shape, and the cell layer had no particular organization. Extracellular matrix (fibronectin, type I collagen, osteopontin) and cytoskeletal protein (actin, vinculin) orientation reflected the cell layer organization. In our experiment human osteoblasts expressed α3β1 integrin but not α2β1 integrin. In addition to currently analyzed roughness magnitude parameters, we calculated roughness organization parameters (fractal dimension parameters) of the substrates. We observed lower adhesion and proliferation on less organized surfaces (i.e., sandblasted ones). The significant statistical correlation observed between fractal dimension parameters (describing surface roughness organization) and cell parameters adds a new concept to the studies of substratum roughness influence on cell behavior. An attempt at modelization of the cell–surface interaction was made that includes the influence of fractal dimensions parameters.

Key words: cell adhesion; vinculin; β1 integrin; roughness characterization; fractal dimension; human osteoblasts

INTRODUCTION

Cell adhesion is a fundamental process directly involved in cell growth, cell migration, and cell differentiation. Adhesion is involved in embryogenesis, maintenance of tissue integrity, wound healing, immune response, cancer metastasis, and biomaterial tissue integration.[1–4] Numerous proteins are involved in cell adhesion: extracellular matrix proteins (fibronectin, collagen, laminin, vitronectin),[4–8] cytoskeletal proteins (actin, talin, vinculin),[9,10] and membrane receptors (integrins).[1,11] Interactions between these proteins and their specific receptors induce signal transduction and consequently influence cell growth and differentiation.[2] The expression of integrins by bone cells *in vitro* and *in vivo* was recently described.[12–14]

The development of bone–implant interfaces depends on the direct interactions of bone matrix and osteoblasts with the biomaterial. Osteoblast adhesion is therefore essential for bone–biomaterial interactions. Early *in vitro* studies of osteoblast–biomaterial interaction were essentially concerned with the effect of diverse materials without any surface characterization on cell proliferation and differentiation.[15] However, it is now understood that the surface properties of biomaterials play a critical role in the establishment of cell–biomaterial interfaces. *In vitro* cytocompatibility studies are increasingly concerned with the influence of surface topography,[16–18] surface charge,[19–21] and consecutive adsorption of proteins[7,8,22–26] on cell attachment and proliferation. Many studies demonstrate that the surface topography is an important parameter to consider.[27–30] However, surface topography is generally poorly described. It is now increasingly admitted that roughness must be considered in terms of amplitude and organization.[31] Previous works illustrated that the amplitude and organization of roughness concomitantly influence cell behavior. On smooth surfaces the bone cells were randomly oriented, although they were lined up parallel to the grooves in an end to end fashion in 5 μm deep grooves. In contrast, they did "ignore" the surface to-

Correspondence to: Dr. K. Anselme
Contract grant sponsor: Fédération Biomatériaux Nord/Pas-de-Calais.

pography on a 0.5-μm grooved surface.[32] In this study we used an original method (fractal analysis) to determine quantitative parameters describing not only roughness amplitude but also roughness organization.[33]

Recent reports examined cell adhesion on materials having various surface properties.[34–38] Some of these studies focused on integrins involved in the modulation of osteoblast adhesion on biomaterials.[4,38] However, the qualitative observations of proteins involved in osteoblast adhesion was not correlated with a quantitative evaluation of adhesion. Moreover, few works attempted to correlate a quantitative evaluation of cell adhesion with roughness parameters of the substratum.[37]

In this article we associate three different studies: one extensively stating the surface roughness of the tested orthopedic metallic surfaces (Ti6Al4V alloy) with usual and original parameters, one quantitatively assessing the adhesion of human osteoblasts on these surfaces using a specific enzymatic detachment assay, and another illustrating the adhesion proteins expressed by human osteoblasts on these various topographies by a qualitative immunostaining using specific antibodies. The results of these three studies are correlated and discussed to make conclusions about the effects of surface roughness of a Ti6Al4V alloy on human osteoblast adhesion.

MATERIALS AND METHODS

One hundred eighty disks of a Ti6Al4V alloy (medical quality; 14-mm diameter, 2-mm height) were processed by sandblasting (500-μm or 3-mm alumina particles) or mechanical polishing (with P4000, P1200, or P80 silicon carbide paper). Thirty-six disks of each treatment were prepared. Metallic substrates were rinsed twice in absolute alcohol and once in demineralized water in ultrasound before 180°C heat sterilization. Seventy-five round glass coverslips (14-mm diameter, 0.13–0.16-mm height, Fisher Scientific, Elancourt, France) were used as controls.

Cell culture

Human bone cells were obtained from explants of trabecular bone from the iliac crest of a 9-year-old patient. After primary culture the cells were frozen in liquid nitrogen and stored. After thawing the cells were cultured in Dulbecco's modified Eagle's medium (DMEM, Eurobio, Les Ulis, France) containing 10% fetal bovine serum (FBS) and 1% penicillin-streptomycin in 75-cm^2 flasks until confluence. After trypsinization (second passage) the cells were harvested and inoculated on metallic disks in 24-well plates.

The osteoblastic characterization of cells was determined after 1,25 (OH)2 vitamin D3 [1,25(OH)2D3] stimulation. Confluent cultures were treated with 10 n*M* [1,25(OH)2D3] for 48 h. The media were removed and the cells were harvested by trypsination. The alkaline phosphatase activity of the lysed cells was measured as described by Lu et al.[39] The osteocalcin content of the conditioned medium and procollagen type I synthesis were determined as described by Lu et al.[39] at the second passage before inoculation onto the metal substrates. These were 389.3 U/g of protein, 2.8 p$M/10^6$ cells, and 1.8 mg/10^6 cells, respectively.

Cell morphology

Cell layers were fixed in 2% paraformaldehyde (w/v) in monosodic dipotassic 0.2*M* buffer, rinsed in monosodic dipotassic 0.175*M* buffer, dehydrated in graded alcohol, critical-point dried with CO_2 (Emscope CPD 750, Elexience, Paris), sputter coated (Emscope SC 500, Elexience), and examined using a Hitachi S520 scanning electron microscope at an accelerating voltage of 25 kV (Elexience).

Immunohistochemistry

Cells were inoculated on the substrates at 1.5×10^4 cells/well in DMEM containing 10% FBS and 1% penicillin-streptomycin. Thirty samples of each material and each surface roughness were inoculated with cells (10 for each incubation period of 24 h, 7 days, and 14 days). Following the incubation period the substrates were rinsed with phosphate buffered saline (PBS, without calcium and magnesium chloride). Cells were fixed for 20 min in 2% paraformaldehyde in monosodic dipotassic 0.2*M* buffer at room temperature followed by three rinses with PBS. Cells were permeabilized with 0.2% (v/v) Triton-X100 (Sigma, L'Isle d'Abeau, France) for 15 min at room temperature followed by three rinses with PBS. Nonspecific binding sites were blocked by incubating the samples in 1% (w/v) bovine serum albumin in PBS for 20 min at room temperature. Cells were stained for proteins involved in cell adhesion (adhesion proteins) for 1 h at room temperature in a humidified atmosphere followed by three rinses with PBS. Various antibodies against adhesion proteins were used: rabbit anti-human fibronectin IgG fraction (1:100; Institut Pasteur, Lyon, France), rabbit anti-human type I collagen IgG fraction (1:100, Institut Pasteur), rabbit polyclonal anti-human osteopontin antibody (1:200, a generous gift from P. Marie, Hôpital Lariboisière, Paris), mouse monoclonal anti-human vinculin (1:200, Sigma), mouse monoclonal anti-human β1 integrin subunit (1:200, Affiniti, Nottingham, U.K.), and anti-α2 and anti-α3 integrin subunits (1:50, Novocastra, Newcastle upon Tyne, U.K.). F-Actin microfilaments were directly revealed by FITC-conjugated phalloidin (25 μg/mL; Sigma). As controls, mouse IgG (1:100, Sigma) or nonimmune rabbit serum (1:100, Institut Pasteur) and PBS were used as primary antibodies.

Cells were fluorescently labeled by incubation with fluorescein-conjugated antibody: FITC-anti-mouse IgG antibody (Caltag, CA, USA) or FITC-anti-rabbit IgG antibody (Sigma)

were used for 45 min at room temperature in a humidified atmosphere followed by three rinses with PBS. The substrates were mounted on a microscope slide under glass coverslips using glycerine/PBS (50/50) containing 1,4-diazobicyclo-(2,2,2,)-octane (25 mg/mL, Sigma) for photobleaching reduction.

The labeled cells were examined using a Zeiss Axioskop microscope (Zeiss, Le Pecq, France) equipped for epifluorescence.

Quantitative adhesion test

Thirty samples of each surface were inoculated with 2×10^4 cells/sample. Five samples were analyzed after each incubation period of 24 h, 3 days, 7 days, 14 days, and 21 days. The cells were enzymatically detached from the samples by a diluted trypsin-EDTA [0.025% (v/v)] treatment. Cells detached after 5, 10, 20, 30, and 60 min were counted with a Coulter Z1 (Coultronics, Margency, France). The remaining cells were detached by a 15-min treatment with nondiluted trypsin-EDTA. The curve of the percentages of released cells versus trypsination time was established. The area included between the curve and the *X* axis was evaluated by integration. The areas obtained were considered as a detachment index that was inversely proportional to the cell adhesion on the biomaterial.[40] The cell proliferation curves on the different materials were drawn from the total detached cell count obtained at each delay during the adhesion test.

Roughness measurement

Six 3-dimensional surfaces were measured using a confocal microscope laser (Lasertek, Elexience, Paris, France) on five samples for the five types of roughness. The 3-dimensional surfaces were discretized into 1024 × 256 points that gave a scanning surface of 60 μm^2. Surfaces were straightened up using the least squares method and no filtering. These data were used to analyze surface topographies. Then some usual and some original roughness parameters were computed. A statistical analysis of the roughness effects on cell proliferation and cell adhesion were performed using SAS© software (SAS Institute, Cary, NC).

X-ray diffraction analysis

To know whether any structural transformation had been processed during surface elaboration, an X-ray diffraction analysis was performed on each sample with a D5000 Siemens diffractometer (Bruker, Wissembourg, France) with a Cu anticathode.

RESULTS

Cell morphology

On the glass samples the flattened cells adhered at 24 h, although there were relatively few. After 7 days the cell layers were not confluent. After 14 days a confluent cell layer covered the samples. The cells appeared to be flattened and oriented in a parallel way. A dense matrix was observed under the cell layer [Fig. 1(a)]. On P4000 polished Ti6Al4V surfaces the same aspects were observed except that after 14 days the extracellular matrix under the cell layer was not so visible [Fig. 1(b)]. On P80 and P1200 polished Ti6Al4V surfaces after 7 and 14 days the cell layers covered the residual grooves of the polishing [Fig. 1(c, d)]. However, no correlation was observed between the orientation of the grooves and the orientation of the cells. On 500-μm and 3-mm sandblasted Ti6Al4V surfaces the cell layers never attained confluence even after 14

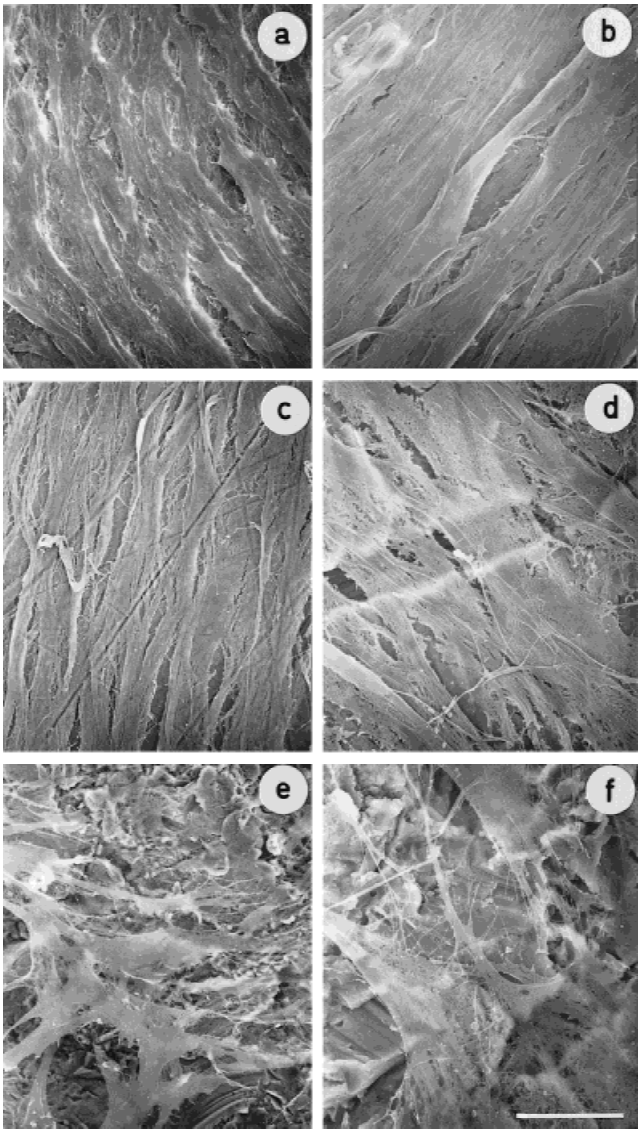

Figure 1. Scanning electron micrographs of human osteoblast cultures on tested samples after 14 days on (a) glass (scale bar = 60 μm), (b) P4000 (scale bar = 15 μm), (c) P1200 (scale bar = 60 μm), (e) 500 μm (scale bar = 60 μm), (f) 3 mm (scale bar = 15 μm), and (d) after 7 days on P80 (scale bar = 15 μm).

TABLE I
Semiquantitative Evaluation of Immunolabelings

		Fibronectin	Type I Collagen	Osteopontin	Actin	Vinculin	β1 Integrin Subunit	α3 Integrin Subunit	α2 Integrin Subunit
Rough	24 h	++++	+++	++	++++	++	+(+)	(+)	—
Ti6A14V	7 days	++++	+++(+)	++(+)	++++	++	+	(+)	—
surfaces	14 days	++++	+++	+++	++++	(+)	+	+	—
Polished	24 h	++++	+++	++	++++	++	+(+)	(+)	—
Ti6A14V	7 days	++++	+++(+)	+(+)	++++	++(+)	+	+	—
surfaces	14 days	++++	+++	+++	++++	(+)	+	+	—
Glass	24 h	+++(+)	++	+++	++++	++	+(+)	—	—
	7 days	+++(+)	++(+)	+++	++++	++(+)	+(+)	+	—
	14 days	+++(+)	+++	+++	++++	—	+(+)	+	—

days. Cells had a stellate shape with numerous filamentous extensions [Fig. 1(e, f)].

Immunohistochemistry

A semiquantitative evaluation of the immunolabeled cells as a function of time is presented in Table I. The main differences among the materials concerned the intensities of the labeling of adhesion proteins and the duration of their presence during the growth of the cell layer. The extracellular matrix was better organized and orientated on smooth surfaces than on rough surfaces. Few differences could be observed on fibronectin, osteopontin, and type I collagen expression among surfaces at the same time points [Fig. 2(a–f)]. On the other hand, a slight increase in osteopontin and type I collagen synthesis was visible as a function of time (Table I). Histochemical staining of F-actin revealed differences in cell orientation on the various substrates, as well as differences in the organization of the cytoskeleton. On smooth surfaces the cells contained many thick stress fibers in a parallel arrangement. The microfilament system organization ran parallel to the previously described general cell morphology. On rough surfaces the microfilament system appeared oriented in the direction of the long axis of the cells, although the cells did not have any particular orientation. Some microfilaments revealed by phalloidin were visible at the cell periphery [Fig. 2(g, h)] and could be related to filamentous extensions previously described on scanning electron micrographs (Fig. 1).

Anti-vinculin immunostaining revealed short, thick, and dense patches considered as focal contacts. The focal contact distribution illustrated the mode of adhesion of osteoblasts on the various surface roughnesses. On smooth surfaces the focal contacts were evenly distributed on all the membrane surfaces that were in contact with the substratum [Fig. 3(a, c, e)]. On rough surfaces the focal contacts were visible only on the extremities of cell extensions where cell membranes were in contact with the substratum [Fig. 3(b, d, f)]. No differences in focal contact distribution were observed with the time in culture, although the vinculin immunolabeling intensity diminished on all the surfaces after 14 days of culture (Table I). The orientation of the vinculin patches seemed to coincide with the orientation of the stress fibers (Figs. 2, 3).

The β1 integrin subunits were also expressed by osteoblasts on various substrates and appeared as thin focal contactlike patches, as well as thin filaments [Fig. 4(a, c)]. Their orientation also coincided with the ori-

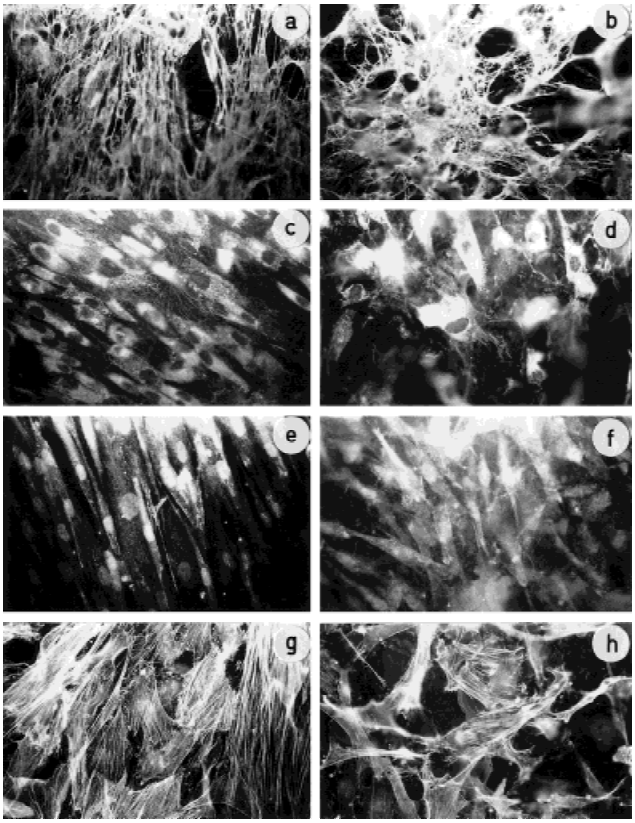

Figure 2. The expression by human osteoblasts of (a, b) fibronectin, (c, d) type I collagen, (e, f) osteopontin, and (g, h) F-actin on (a, c, e, g) smooth Ti6Al4V surfaces and (b, d, f, h) rough Ti6Al4V surfaces (original magnification ×100).

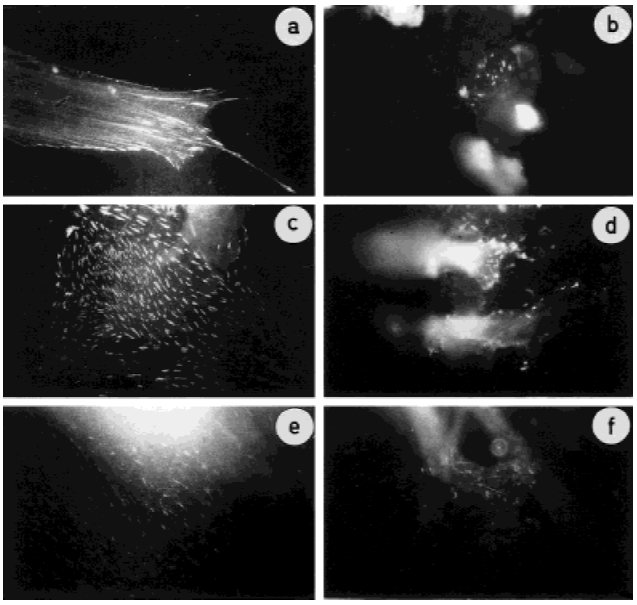

Figure 3. The expression of vinculin after (a, b) 1 day, (c, d) 7 days, and (e, f) 14 days of culture on (a, c, e) smooth Ti6Al4V surfaces and (b, d, f) rough Ti6Al4V surfaces (original magnification ×250).

entation of the stress fibers (i.e., with the long axis of the cells). No qualitative or quantitative modification of β1 integrin subunits expression was observed between 24 h and 7 days of culture. On the other hand, a decrease of the intensities of the immunolabel was noted at 14 days on all surfaces (Table I). The α2 integrins were not expressed by the cells based on our failure to detect any immunolabel using an anti-α2 integrin subunit antibody. When using an anti-α3 integrin subunit antibody we obtained a pericellular membrane labeling after 14 days of culture. Sometimes the label was also noted intracellularly in cells cultured on the substrates. This labeling appeared to be specific because the immunofluorescence was significantly different from that noted in the controls using mouse IgG (Fig. 5).

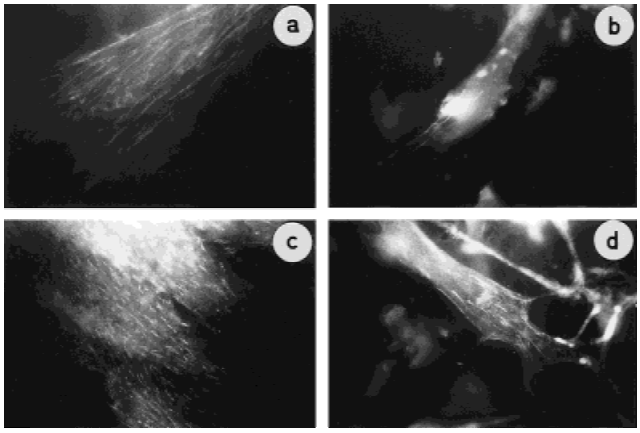

Figure 4. The expression of the β1 integrin subunit after (a, b) 1 day and (c, d) 7 days on (a, c) smooth Ti6Al4V surfaces and (b, d) rough Ti6Al4V surfaces (original magnification ×250).

Quantitative adhesion tests

A statistical comparison of cell adhesion as a function of time showed that for most surfaces the adhesion was not affected during the first week of culture but increased after 14 days. For P4000, P80 polished, and 500-μm sandblasted Ti6Al4V surfaces there was also an increase of adhesion between 14 and 21 days of culture, although for P1200 polished Ti6Al4V substrates and glass the adhesion after 21 days did not increase compared to 14 days of culture. For 3-mm sandblasted Ti6Al4V samples there was no difference of adhesion whatever the time of culture. The adhesion remained weak.

An intersurfaces statistical comparison demonstrated that at each time the adhesion was weaker on glass than on metallic substrates. After 1 day the adhesion on 500-μm sandblasted, P4000, and P1200 polished Ti6Al4V samples was stronger than on other surfaces. After 3 days the adhesion was comparable on all metallic substrates. After 7 days the adhesion on metallic substrates was significantly stronger on 500-μm sandblasted Ti6Al4V samples compared to all surfaces except P1200 polished Ti6Al4V samples. After 14 days the P1200 polished Ti6Al4V surfaces were the most favorable surfaces for osteoblast adhesion. Weaker adhesion was obtained on glass and 3-mm sandblasted Ti6Al4V samples. After 21 days this result was maintained but the differences of adhesion between glass and 3-mm sandblasted Ti6Al4V samples and the other surfaces were increased compared to 14 days of culture (Fig. 6).

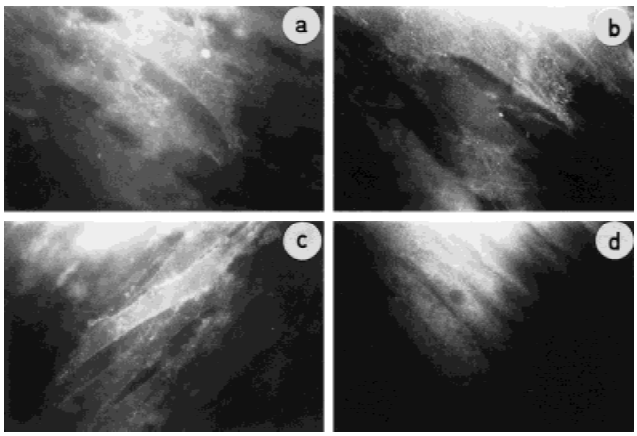

Figure 5. The expression of the α3 integrin subunit after (a, b) 7 days and (c) 14 days on (a, b) smooth Ti6Al4V surfaces and (c) rough Ti6Al4V surfaces. (d) The negative control using 1:100 diluted mouse IgG after 14 days of culture on glass surfaces (original magnification ×250).

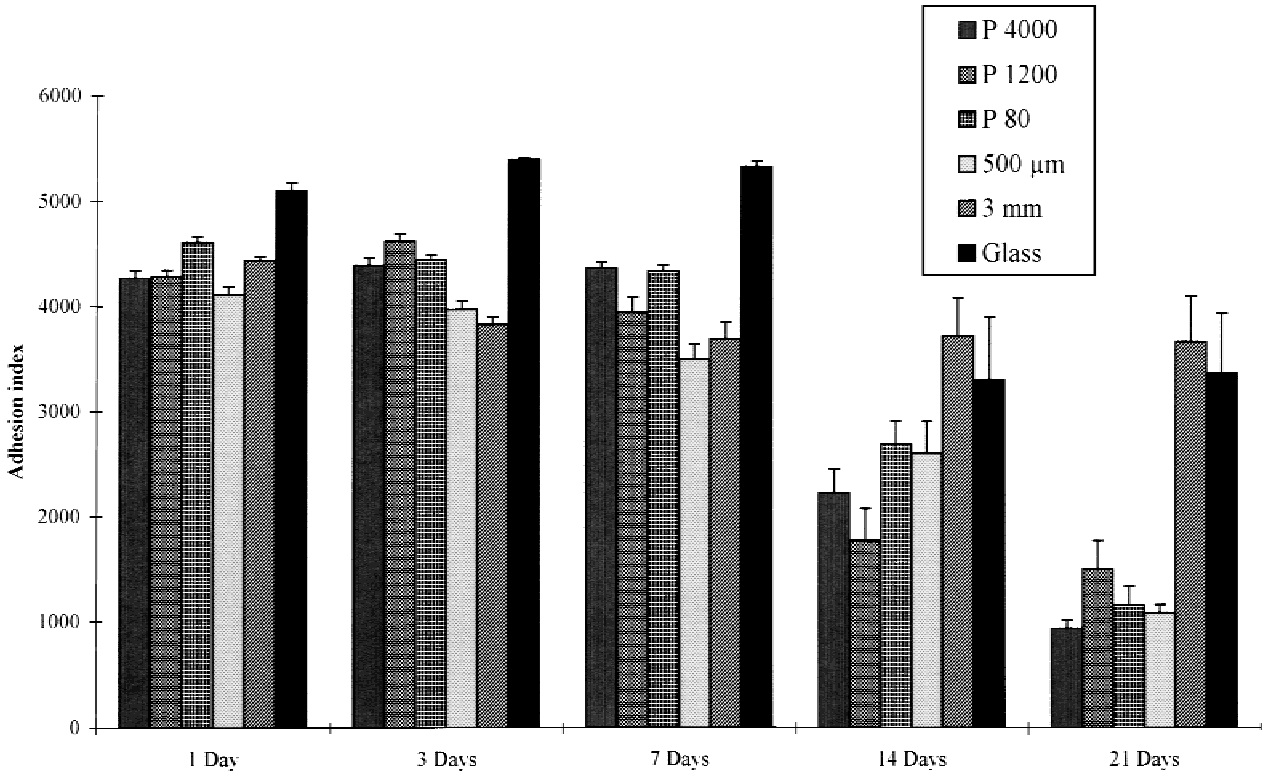

Figure 6. A detachment index histogram on the various tested surfaces as a function of time.

Cell proliferation

The proliferation on Ti6Al4V samples decreased when the average surface roughness (R_a) increased (Table II). The proliferation was higher on smooth samples than on rough samples (Fig. 7).

Roughness measurement

Roughness parameters were computed (Table II). Figure 8 describes the qualitative surface aspects of the Ti6Al4V test samples. The roughness of the samples was in the following order: P4000 < P1200 < P80 < 500 µm < 3 mm. On P1200 and P80 polished samples the residual grooves after polishing were discernible.

Statistical analysis

A rough surface can be defined by a great number of parameters. One hundred one parameters were calculated using an original computer program. We chose to focus on those parameters whose influence was the most evident with respect to cell response. If two parameters had the same statistical influence, we kept those parameters that affected cell adhesion or cell proliferation.

Cell proliferation

Cell proliferation equation.

Cell proliferation did not obey a linear relation with time in culture. For example, we plotted the curve of cell proliferation versus time for the P4000 roughness

TABLE II
Statistics of Roughness Measures on Samples

	R_a (µm)	R_t (µm)	R_{t+} (µm)	R_{t-} (µm)	SK (µm)	EK (µm)	Δ	Surf (%)
Polished								
4000	0.16	2.53	1.26	−1.27	−0.30	11.38	2.22	2.07
1200	0.20	3.30	1.29	−2.01	−1.78	16.49	2.27	2.33
80	0.30	3.30	1.94	−1.36	−0.04	6.42	2.24	2.52
Sandblasted								
500 µm	2.19	16.08	10.63	−5.46	0.74	4.34	2.38	96.57
3 mm	3.40	24.76	16.28	−8.42	0.98	4.89	2.47	299

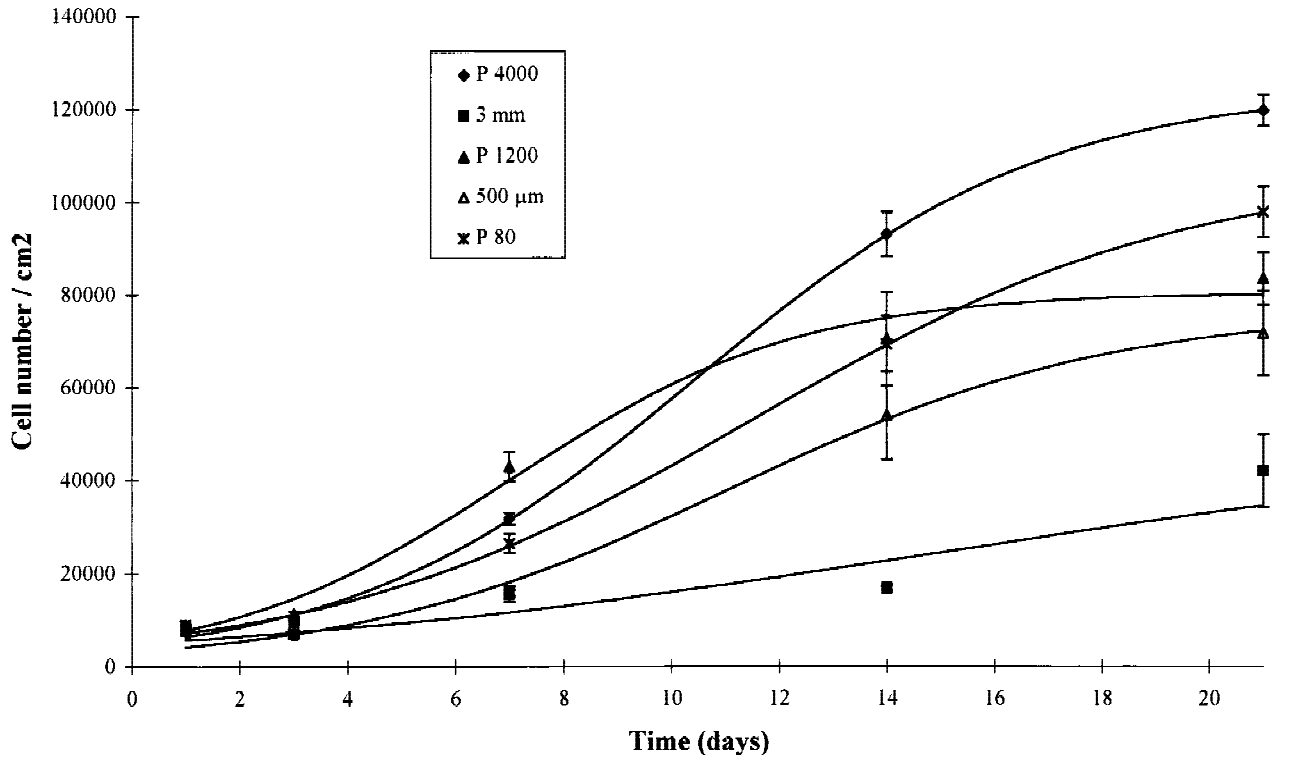

Figure 7. Proliferation curves on the various tested surfaces as a function of time. The curves were established using Equation (1) (cf. text) obtained by a nonlinear least squares method. They showed good accuracy with the experimental data.

sample (Fig. 7). The linear relation was visually rejected. To analyze the effect of the roughness on cell proliferation an appropriate statistical model of cell proliferation versus time in culture had to be formulated. This equation must model cell proliferation with a minimal number of coefficients and each coefficient had to describe independent biological phenomena. After various statistical models adjustments the cell proliferation $P(t)$ as a function of time t could be modeled for a given roughness through the following equation:

$$P(t) = \frac{\alpha_0}{1 + \exp(-\alpha_1(t - t_0) - \alpha_2)}, \quad (1)$$

where α_0, α_1, and α_2 are constants determined by the nonlinear least squares method; t_0 is the time of the first cell count after cell deposition; α_0 is the maximal threshold of the cell proliferation; α_1 is the effect of time on cell proliferation (the greater the α_1 the faster the cell proliferation and the faster the maximal threshold of the cell proliferation is reached); and α_2 is the influence of the initial number of cells on cell proliferation. We observed that the experimental data correlated well with the modeled results (Fig. 7).

Roughness effects on cell proliferation.

As shown in Table II, the fractal dimension discriminated the cell proliferation very well. We noticed that cell proliferation underwent a progressive increase according to the fractal dimension (Δ). The greater the fractal dimension, the more chaotic the surface.[33] When the surface is very ordered, $\Delta = 2$. If the surface is chaotic, then $\Delta = 3$. We analyzed the adequacy between the cell proliferation after 21 days and the R_a parameter and the fractal dimension. Then we obtained a better correlation coefficient when we used the fractal dimension ($R = 0.94$) rather than the R_a (0.89). As a result, Equation (1) was modified to introduce the surface roughness via the fractal dimension.

We then postulated that cell proliferation could be modeled by the following equation:

$$P(t,\Delta) = \frac{\beta_1(\Delta - 2)H(t,t_0) + \beta_2}{1 + \exp[\beta_3(t - t_0) + \beta_4]}. \quad (2)$$

In the Equation (2) the coefficients also get some physical information. A new parameter β_1 was introduced to take the roughness effect into account. The greater this parameter was, the more influential was the effect of surface organization on cell proliferation. If the surface was not chaotic, then $\Delta = 2$ and Equation (3) could be reduced to Equation (1). The β_2 represented the maximal threshold of the cell proliferation if the surface was ordered ($\Delta = 2$), β_3 represented the effect of time on the cell proliferation rate, and β_4 represented the influence of the initial number of cells at $t = t_0$ and was independent of the surface roughness.

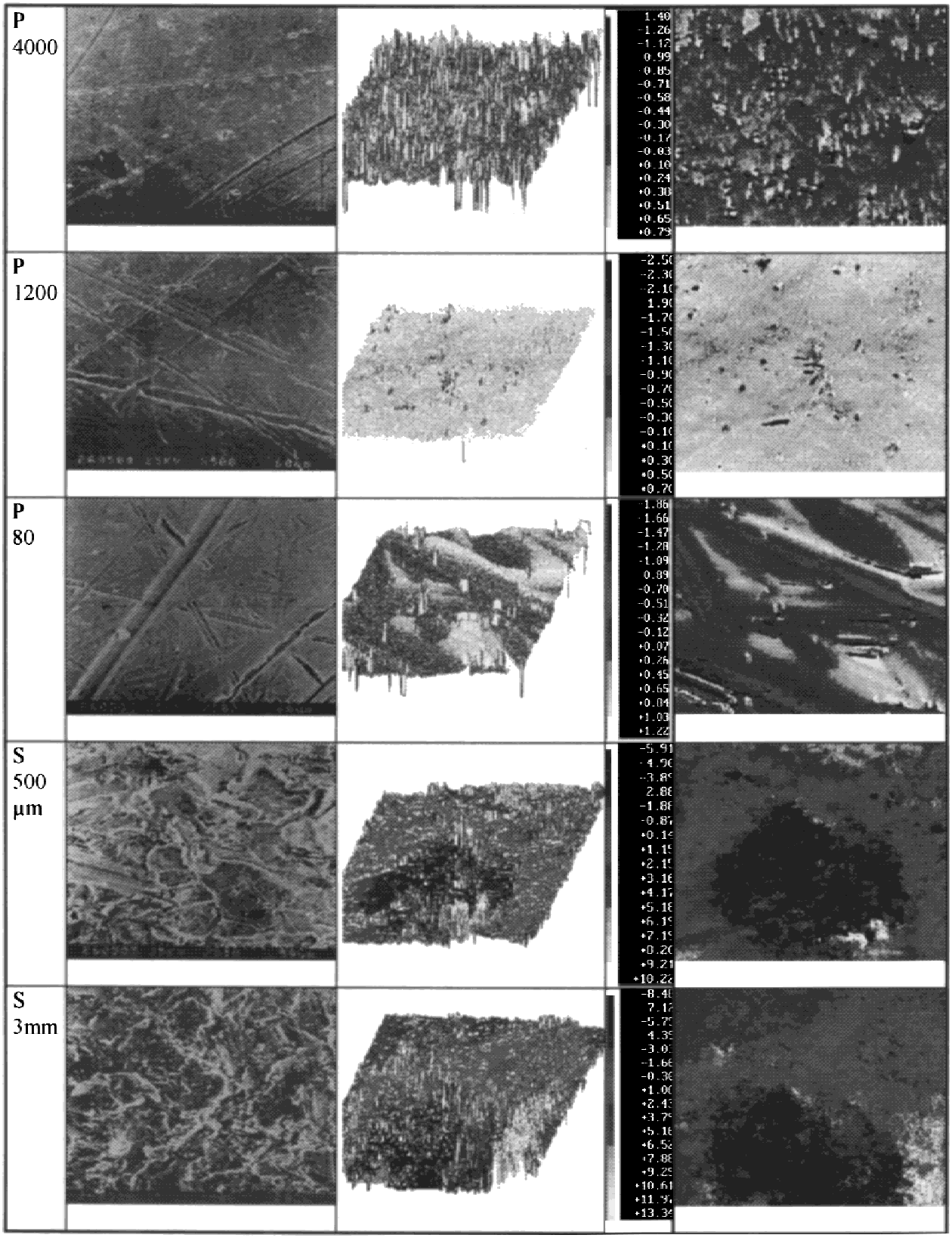

Figure 8. The roughness surfaces of the samples. The scanning electron microscopy photographs are on the left, the 3-dimensional scanning surfaces are in the center, and the surface topography is on the right. The scales of the roughness magnitudes are in microns (μm).

By using a nonlinear least square method we demonstrated that all coefficients were highly significant, which meant that this model described the cell proliferation well and had good accuracy with the experimental data corresponding to a correlation coefficient of 0.98 (Fig. 9).

To help with the interpretation of the negative relation between the fractal dimension and cell proliferation, we postulated that the contact area between a cell and a surface may be modeled by the following equation:

$$A \propto \frac{P}{E} \frac{\lambda_c^{\frac{(3-\Delta)}{2}}}{\lambda_r^{\Delta-2}}, \tag{3}$$

where A is the contact area between the cell and the substrate surface, P is the applied extended loading, E is the Young's modulus of the cell membrane, $1/\lambda_r$ is the minimal contact length necessary to allow cell adhesion on the material surface, and $1/\lambda_c$ is the maximal cell size. From this equation we can observe that the more the fractal dimension of the surface increases, the more the contact surface between cells and substrate decreases. This may explain the decrease of cell proliferation when the fractal dimension (Δ) increases.

Cell adhesion

The same modelization attempt was done using our adhesion parameter (i.e., the detachment index). The lower the detachment index, the greater the cell adhesion. When using an analysis of variance on experimental data with the culture duration and the surface roughness, culture duration proved to be the main influencing factor on cell adhesion.

To modelize the detachment index with the culture duration for a given roughness, we chose the following equation:

$$A(t) = \frac{\alpha_0}{1 + \exp(\alpha_1(t - t_0) - \alpha_2)}. \tag{4}$$

where $A(t)$ is the detachment index. Thereafter, we introduced a roughness parameter in the equation. The roughness parameter should include the phenomena about the 3-mm sandblasted surface. If we analyzed Table II, the criteria developed surface (Surf) discriminated the roughness of 3-mm sandblasted surfaces.

Cell adhesion was then modelized by the following equation:

$$A(t,\text{Surf}) = \frac{\alpha_0}{1 + \exp[\alpha_1(t - t_0) + \alpha_2(t - t_0)(\text{Surf}) + \alpha_3]}. \tag{5}$$

By using a nonlinear least squares method we demonstrated that all coefficients were highly significant, which meant that this model described the cell proliferation well and had good accuracy with the experimental data corresponding to a correlation coefficient of 0.96 (Fig. 10).

The coefficients α_0 and α_3 represented the initial cell adhesion strength, α_1 represented the cell adhesion strength during the time in culture, and the α_2 coefficient represented the roughness influence on the cell adhesion and this influence depended on the time in culture. Because the α_2 coefficient was highly signifi-

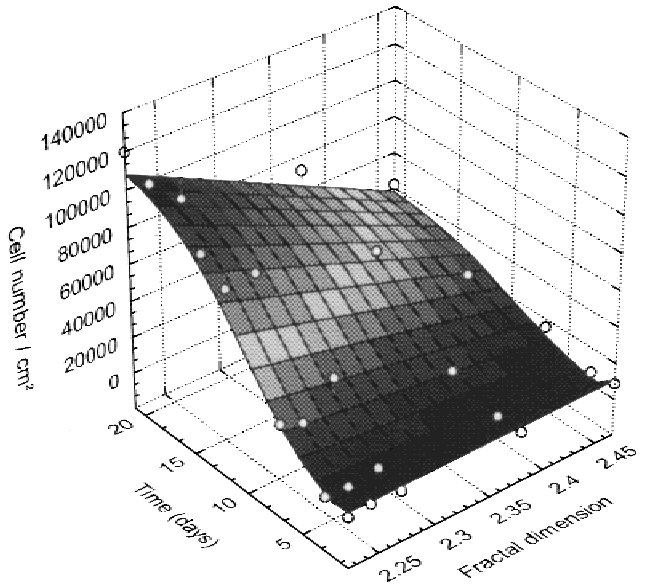

Figure 9. The cell proliferation versus time in culture and versus the fractal dimension (Δ).

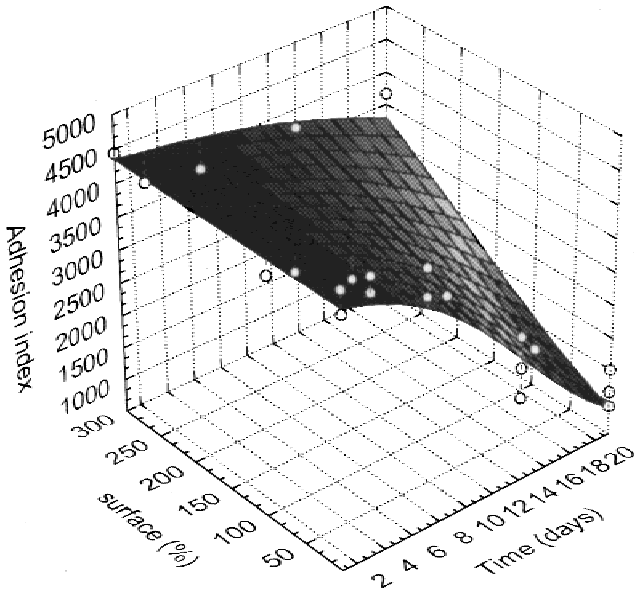

Figure 10. The cell adhesion versus the developed surface and versus time.

cant, we concluded that the cell detachment index was higher on surfaces with higher developed surface; this relation increased with the time in culture. One hypothesis may be that when the developed surface increased the fractal aspect of the surface increased and that, consequently, relating to Equation (3), cells may have some difficulties in finding enough fixation sites.

Surface analysis by X-ray diffraction method

The same number of peaks appeared in all the diffractograms (not shown). This means that the surfaces got the same chemical and structural properties.

DISCUSSION

Few studies attempted to correlate a quantitative evaluation of cell adhesion and an extensive description of topographical and physicochemical aspects of surfaces. Lampin et al. studied chick embryo vascular and corneal cell adhesion on poly(methyl methacrylate) substrates with varying surface topographies. A particular effort was made to precisely describe roughness and surface free energy of substrates.[37] Contrary to them, we observed a negative statistical correlation between the adhesion and the developed area.

The fractal dimension Δ parameter was previously demonstrated as a parameter that describes surface organization.[33] The higher the Δ parameter, the lower the surface organization. Our results showed a lower proliferation on less organized surfaces (i.e., sandblasted ones). The significant correlation we observed between the Δ parameter and cell proliferation adds a new concept to the studies of substratum roughness influence on cell behavior. We demonstrated and modelized the statistical influence of the fractal dimension and the percent of the developed surface on cell proliferation and cell adhesion, respectively. To interpret this influence, we attempted to modelize the contact area between a cell and a substrate surface by including the fractal dimension in the equation. From this equation we observed that the more the fractal dimension increased, the more the contact area between the cell and substrate decreased. This interpretation is consistent with our experimental results. Although the experimental effect of surface roughness on cell adhesion was demonstrated mainly on the most extreme surfaces like glass and 3-mm sandblasted titanium alloy, the statistical analysis demonstrated the high significant correlation between the surface roughness (percent of developed surface) and the cell adhesion (detachment index).

Using an anti-vinculin antibody we observed that on rough surfaces vinculin labeled focal contacts were less numerous than on smooth surfaces because they were observed only on the extremities of cell extensions where cell membranes were in contact with the substratum. Other authors also previously demonstrated a reduced number and reduced size of adhesion plaques of cells on surfaces less favorable for cell attachment and cell proliferation.[35] Consequently, cell adhesion and cell proliferation may be impaired on more chaotic surfaces. This was confirmed by observations of many authors. The cytocompatibility of smooth surfaces of a Co-Cr alloy was better when compared to rough surfaces.[16] Rough titanium surfaces appeared to decrease the proliferation and alkaline phosphatase activity of adult human bone cells compared to smooth titanium surfaces.[30] Proliferation of a human osteosarcoma cell line (MG-63) decreased with increasing surface roughness, although collagenous protein production decreased on smooth surfaces and PGE2 and TGFβ1 production increased on rough surfaces.[27–29]

Morphologically, cell layer organization was modified by the roughness of the underlying substrates. Sandblasted surfaces provoked the disorganization of cell layers. Moreover, confluence was not attained on these surfaces. Cells on polished surfaces attained confluence and were organized in a parallel order as they do on glass or on a plastic culture dish. Contrary to results obtained with human gingival fibroblasts[18,41] or with osteoblastic cells,[33] the depth of the residual grooves of between 2.5 and 3.3 μm on polished materials in our experiment was insufficient to influence human osteoblasts, perhaps because of the absence of the orientation of the residual grooves.

Immunolabelings also revealed a differential organization of extracellular matrix proteins on rough and smooth surfaces that correlated with the cell layer organization. We observed an expected tight correlation between the orientation of the cytoskeletal F-actin network and vinculin labeled patches. Vinculin is effectively involved in the attachment of actin-containing stress fibers to the plasma membrane on the cytoplasmic side of adhesion plaques.[9,10] The colocalization of vinculin and β1 integrin that we observed may be explained by the intermediate talin protein that is known to bind to both integrin and vinculin.[9] The focal contactlike patches aspect of the β1 subunits that we observed was also described by Sinha and Tuan.[38] The expression of α3 integrin associated with β1 integrin from 7 days indicates that the human osteoblasts in our experiment expressed the multifunctional receptor $\alpha3\beta1$ integrin that binds to fibronectin, collagen, and laminin.[1] This could be related to the relatively high expression of fibronectin by the cells. Many authors described the *in vitro* expression of the α2 subunit by human osteoblasts using Western blotting,[4]

flow cytometric analysis,[14] or immunofluorescence methods.[12,38] Our negative results could be related to the weak type I collagen expression we obtained, because α2β1 integrin is a more specific receptor for collagen than α3β1 integrin.[1]

Our quantitative method for adhesion evaluation has shown its efficacy to discriminate the cell adhesion on the same materials with various surface roughnesses or to compare cell adhesion on different materials. Moreover, the modifications of cell adhesion during cell growth highlight the influence of diverse phenomena involved in adhesion at different stages after cell attachment. In the first 24 h after cell inoculation the cells attached at the material surface by physicochemical interactions mediated by calcium and magnesium ions and adsorptions of serum vitronectin.[19,20] A cell–material interface was established. After this delay the adhesion of the cells was mediated by the extracellular matrix; they were synthesized on the surface through specific integrins and to specific sites on these proteins (RGD sequences)[1,4]: a cell–matrix–material interface was a concern. As Steele et al. noted, the initial cell attachment evaluation would be of limited value as an end point for a screening assay of potential material surfaces.[20] The adhesion measurement we did after 3, 7, 14, and 21 days evaluated the strength of the cell–matrix–material interface. Because this strength essentially depends on the matrix organization, we attempted to correlate morphological observations with quantification of cell adhesion. The matrix organization after 7 and 14 days was effectively disturbed on rough surfaces compared to smooth surfaces. On the other hand, in an interdelay comparison on each surface no modifications of extracellular matrix protein expression were observed from 7 days. Only integrin and vinculin expression decreased after 14 days compared to 7 days after inoculation. Either these proteins were really less expressed or the thickness of the confluent cell layer attenuated the fluorescent signal. Because the modification of the adhesion occurring between 7 and 21 days of culture may be related to a maturation of extracellular matrix and/or to a maturation of cell–matrix interactions, further quantitative screening of adhesion proteins by biochemical methods is planned to investigate this point.

CONCLUSIONS

We quantitatively evaluated human osteoblast adhesion on metallic substrates with various surface roughnesses at several time points after inoculation and studied its correlation with qualitative modifications of adhesion protein expression. The main differences among samples concerned the cell layer and extracellular matrix organization on polished or sandblasted surfaces. Cells were orientated in a parallel order on polished surfaces. This orientation was not affected by residual grooves after polishing. On sandblasted surfaces the cells never attained confluence and had a stellate shape and the cell layer and extracellular matrix showed an impaired organization. By using an anti-vinculin antibody we observed the less numerous focal contacts of cells on rough surfaces. This observation can be related to the weaker adhesion and proliferation observed on these surfaces.

The quantitative method we developed to evaluate cell adhesion on biomaterials demonstrated its efficacy to discriminate various surface roughnesses on the same material or to compare diverse materials. Moreover, we extensively analyzed the topography of our samples and, in addition to currently analyzed roughness magnitude parameters, we calculated roughness organization parameters (fractal dimension parameters). These fractal dimension parameters correlated statistically with the proliferation of cells and the adhesion index. By means of modelization of the contact area between a cell and a substrate, we demonstrated that the more the fractal dimension of the substrate increased, the more the contact area between the cell and substrate decreased. This is in agreement with our experimental data: a lower adhesion and proliferation on less organized surfaces (i.e., sandblasted ones).

We are now developing investigations to study osteoblast adhesion on surfaces with the same roughness magnitude but with organized and disorganized surfaces to determine the effects of surface roughness organization on cell adhesion. Physicochemical surface analysis will also be performed and correlated with roughness parameters in these further investigations.

The authors thank SH industries (Marly, France) for kindly supplying the Ti6Al4V substrates, Dr. P. Marie for giving us the anti-osteopontin antibody, and Mr. R. Fromentin for preparing the micrographs.

REFERENCES

1. Hynes RO. Integrins: versatility, modulation, and signalling in cell adhesion. Cell 1992;69:11–25.
2. Roskelley CD, Srebow A, Bissell MJ. A hierarchy of ECM-mediated signalling regulates tissue-specific gene expression. Curr Opin Cell Biol 1995;7:736–747.
3. Huttenlocher A, Sandborg RR, Horwitz AF. Adhesion in cell migration. Curr Opin Cell Biol 1995;7:697–706.
4. Gronowitz G, Mccarthy MB. Response of human osteoblasts to implants materials: integrin-mediated adhesion. J Orthop Res 1996;14:878–887.
5. Grzesik WJ, Gehron Robey P. Bone matrix RGD glycoproteins: immunolocalization and interaction with human primary osteoblastic bone cells *in vitro*. J Bone Miner Res 1994;9:487–496.

6. Gehron Robey P, Fedarko NS, Hefferan TE, Bianco P, Vetter UK, Grzesik WJ, Friedenstein A, Van Der Plum A, Mintz KP, Young MF, Kerr JM, Ibaraki K, Heegaard AM. Structure and molecular regulation of bone matrix proteins. J Bone Miner Res 1993;8:S483–S487.
7. Thomas CT, Mcfarland CD, Jenkins ML, Rezania A, Steele JG, Healy KE. The role of vitronectin in the attachment and spatial distribution of bone-derived cells on materials with patterned surface chemistry. J Biomed Mater Res 1997;37:81–93.
8. Howlett CR, Evans MDM, Walsh WR, Johnson G, Steele JG. Mechanism of initial attachment of cells derived from human bone to commonly used prosthetic materials during cell culture. Biomaterials 1994;15:213–222.
9. Burridge K, Fath K. Focal contacts: transmembrane links between the extracellular matrix and the cytoskeleton. Bioessays 1989;10:104–108.
10. Otto JJ. Vinculin. Cell Motil Cytoskel 1990;16:1–6.
11. Horton MA, Davies J. Perspectives: adhesion receptors in bone. J Bone Miner Res 1989;4:803–808.
12. Clover J, Dodds RA, Gowen M. Integrin subunit expression by human osteoblasts and osteoclasts *in situ* and in culture. J Cell Sci 1992;103:267–271.
13. Hughes DE, Salter DM, Dedhar S, Simpson R. Integrin expression in human bone. J Bone Miner Res 1993;8:527–533.
14. Gronthos S, Stewart K, Graves SE, Hay S, Simmons PJ. Integrin expression and function on human osteoblast-like cells. J Bone Miner Res 1997;8:1189–1197.
15. Vrouwenvelder WCA, Groot CG, de Groot K. Histological and biochemical evaluation of osteoblasts cultured on bioactive glass, hydroxyapatite, titanium alloy, and stainless steel. J Biomed Mater Res 1993;27:465–475.
16. Naji A, Harmand MF. Study of the effect of the surface state on the cytcompatibility of a Co-Cr alloy using human osteoblasts and fibroblasts. J Biomed Mater Res 1990;24:861–871.
17. Könönen M, Hornia M, Kivilahti J, Hautaniemi J, Thesleff I. Effect of surface processing on the attachment, orientation, and proliferation of human gingival fibroblasts on titanium. J Biomed Mater Res 1992;26:1325–1341.
18. Murray DW, Rae T, Rushton N. The influence of the surface energy and roughness of implants on bone resorption. J Bone Joint Surg 1989;71B:632–637.
19. Meyer U, Szulczewski DH, Möller K, Heide H, Jones DB. Attachment kinetics and differentiation of osteoblasts on different biomaterials. Cell Mater 1993;3:129–140.
20. Steele JG, Mcfarland CD, Dalton BA, Johnson G, Evans MDM, Howlett CR, Underwood PA. Attachment of human bone cells to tissue culture polystyrene and to unmodified polystyrene: the effect of surface chemistry upon initial cell attachment. J Biomater Sci Polym Ed 1993;5:245–257.
21. Möller K, Meyer U, Szulczewski DH, Heide H, Priessnitz B, Jones DB. The influence of zeta potential and interfacial tension on osteoblast-like cells. Cell Mater 1994;4:263–274.
22. Boyan BD, Hummert TW, Dean DD, Schwartz Z. Role of material surfaces in regulating bone and cartilage cell response. Biomaterials 1996;17:137–146.
23. Shelton RM, Rasmussen AC, Davies JE. Protein adsorption at the interface between charged polymer substrata and migrating osteoblasts. Biomaterials 1988;9:24–29.
24. Ruardy TG, Schakenraad JM, Van Der Mei HC, Busscher HJ. Adhesion and spreading of human skin fibroblasts on physicochemically characterized gradient surfaces. J Biomed Mater Res 1995;29:1415–1423.
25. Healy KE, Thomas CT, Rezania A, Kim JE, Mckeown PJ, Lom B, Hockberger PE. Kinetics of bone cell organization and mineralization on materials with patterned surface chemistry. Biomaterials 1996;17:195–208.
26. Chesmel KD, Black J. Cellular responses to chemical and morphologic aspects of biomaterials surfaces. I. A novel *in vitro* model system. J Biomed Mater Res 1995;29:1089–1099.
27. Martin JY, Schwartz Z, Hummert TW, Schraub DM, Simpson J, Lankford J, Dean DD, Cochran DL, Boyan BD. Effects of titanium surface roughness on proliferation, differentiation, and protein synthesis of human osteoblast-like cells (MG63) J Biomed Mater Res 1995;29:389–401.
28. Kieswetter K, Schwartz Z, Hummert TW, Cochran DL, Simpson J, Dean DD, Boyan BD. Surface roughness modulates the local production of growth factors and cytokines by osteoblast-like MG-63 cells. J Biomed Mater Res 1996;32:55–63.
29. Boyan BD, Batzer R, Kieswetter K, Liu Y, Cochran DL, Szmuckler–Moncler S, Dean DD, Schwartz Z. Titanium surface roughness alters responsiveness of MG63 osteoblast-like cells to 1α,25-(OH)2D3. J Biomed Mater Res 1998;39:77–85.
30. De Santis D, Guerriero C, Armato U, Nocini PF, Richards G, Gotte P. Adult human bone cells from jaw bones cultured on plasma-sprayed or polished surfaces of titanium or hydroxylapatite discs. J Mater Sci Mater Med 1996;7:21–28.
31. Lopez J, Hanseli G, Le Bosse JC, Mathia T. Caractérisation fractale de la rugosité tridimensionnelle de surface. J Phys III France 1994;4:2501–2219.
32. Chesmel KD, Clark CC, Brighton CT, Black J. Cellular responses to chemical and morphologic aspects of biomaterial surfaces. II. The biosynthetic and migratory response of bone cell populations. J Biomed Mater Res 1995;29:1101–1110.
33. Bigerelle M, Iost A. Calcul de la dimension fractale d'un profil par la méthode des autocorrélations moyennées normées (AMN). CR Acad Sci Paris B 1996;323:669–675.
34. Puleo DA, Bizios R. Formation of focal contacts by osteoblasts cultured on orthopedic biomaterials. J Biomed Mater Res 1992; 26:291–301.
35. Hunter A, Archer CW, Walker PS, Blunn GW. Attachment and proliferation of osteoblasts and fibroblasts on biomaterials for orthopaedic use. Biomaterials 1995;16:287–295.
36. Sinha RK, Morris F, Shah SA, Tuan RS. Surface composition of orthopaedic implant metals regulates cell attachment, spreading, and cytoskeletal organisation of primary osteoblasts *in vitro*. Clin Orthop Rel Res 1994;305:258–272.
37. Lampin M, Warocquier–Clerout R, Legris C, Degrange M, Sigot–luizard MF. Correlation between substratum roughness and wettability, cell adhesion, and cell migration. J Biomed Mater Res 1997;36:99–108.
38. Sinha RK, Tuan RS. Regulation of human osteoblast integrin expression by orthopedic implant materials. Bone 1996;18:451–457.
39. Lu JX, Flautre B, Anselme K, Gallur A, Descamps M, Thierry B, Hardouin P. Role of the porous interconnections in porous bioceramics on bone recolonization *in vitro* and *in vivo*. J Mater Sci Mater Med 1999;10:111–120.
40. Anselme K, Lanel B, Gentil C, Hardouin P, Marie PJ, Sigot–luizard MF. Bone organotypic culture method: a model for cytocompatibility testing of biomaterials? Cells Mater 1994;4: 113–123.
41. Meyle J, Gültig K, Wolburg H, Von Recum AF. Fibroblast anchorage to microtextured surfaces. J Biomed Mater Res 1993; 27:1553–1557.